

# Energy Analysis of Multi-Legged Locomotion Systems

Manuel F. Silva <sup>1</sup>, J. A. Tenreiro Machado <sup>1</sup>, António M. Lopes <sup>2</sup>

<sup>1</sup> Institute of Engineering of Porto, Dept. of Electrical Engineering, Portugal  
Rua Dr. António Bernardino de Almeida, 4200-072 PORTO, Portugal  
Email: {mfsilva,jtm}@dee.isep.ipp.pt

Phone: +351 - 22 - 834 05 00

Fax: +351 - 22 - 834 05 39

<sup>2</sup> Faculty of Engineering of Porto, Dept. of Mechanical Engineering, Portugal  
Rua Dr. Roberto Frias, 4200-465 PORTO, Portugal

Email: aml@fe.up.pt

Phone: +351 22 508 17 58

Fax: +351 22 508 14 45

## ABSTRACT

This paper presents the energy analysis of periodic gaits for multi-legged locomotion systems. The main purpose is to determine the system performance during walking and the best set of locomotion variables that minimizes a cost function related to energy. For that objective, the prescribed motion of the robot is completely characterized in terms of several locomotion variables such as gait, duty factor, body height, step length, stroke pitch, maximum foot clearance, link lengths, body and legs mass and cycle time. In this work, we formulate three indices to quantitatively measure the performance of the walking robot namely the mean absolute power, the mean power dispersion and the mean power lost in the joint actuators. A set of experiments reveals the influence of the locomotion variables in the proposed indices.

## 1 INTRODUCTION

Walking machines allow locomotion in terrain inaccessible to other type of vehicles, since they do not need a continuous support surface. On the other hand, the requirements for leg coordination and control impose difficulties beyond those encountered in wheeled robots (1,2). Gait selection is a research area, requiring an appreciable modeling effort for improvement of mobility with legs in unstructured terrain (3,4,5,6). Previous studies focused in the structure and selection of locomotion modes. Nevertheless, there are different optimization criteria such as energy efficiency, stability, velocity, comfort, mobility and environmental impact (7,8). With these facts in mind, a simulation model for multi-leg locomotion systems was developed, for several periodic gaits. This study intends to generalize previous work (9,10,11) through the formulation of several dynamic indices, measuring the average power during different walking trajectories, the standard deviation of the power consumption and the energy lost in the joint actuators along the walking cycle.

The foot and body trajectories are analyzed in what concerns its variation with the gait, duty factor, step length, maximum foot clearance and body height. Several simulation experiments

reveal the system configuration and the type of the movements that lead to a better mechanical implementation for a given locomotion mode, from the viewpoint of the dynamic indices.

Bearing these facts in mind, the remainder of this paper is organized as follows. Section two introduces the model for a multi-legged robot and the motion planning algorithms. Section three formulates the optimizing dynamic indices and section four develops a set of experiments that reveal the influence of the system parameters in the periodic gaits. Finally, section five presents the main conclusions and directions towards future developments.

## 2 A MODEL FOR MULTI-LEGGED LOCOMOTION

We consider a longitudinal walking system with  $2n$  identical legs ( $n \geq 2$ ), with the legs equally distributed along both sides of the robot body, having each one three rotational joints.

Motion is described by means of a world coordinate system (Fig. 1). Defining the leg lengths  $L_1$  and  $L_2$ , the cycle time  $T$ , the duty factor  $\beta$ , the transference time  $t_T = (1-\beta)T$ , the support time  $t_S = \beta T$ , the step length  $L_S$ , the stroke pitch  $S_P$ , the body height  $H_B$  and maximum foot clearance  $F_C$ , we consider a periodic trajectory for each foot, maintaining a constant body velocity  $V_F = L_S/T$ .

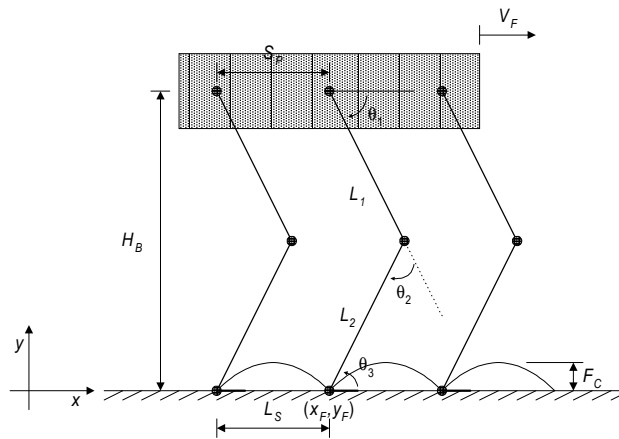


**Fig. 1 Coordinate system and variables that characterize the motion trajectories of the multi-legged robot**

The algorithm for the forward motion planning accepts the body and feet trajectories in  $\{x, y\}$  as inputs and, by means of an inverse kinematics algorithm, generates the related joint trajectories, selecting the solution corresponding to a forward knee.

The body of the robot, and by consequence the legs hips, are assumed to have a horizontal movement with a constant forward speed  $V_F$ . Therefore, the  $\{x, y\}$  coordinates of the hip of the legs are given by (for leg  $i$ ):

$$x_{hi}(t) = V_F \cdot t \quad (1a)$$

$$y_{hi}(t) = H_B \quad (1b)$$

For a particular gait and duty factor  $\beta$  it is possible to calculate (1) for leg  $i$  the corresponding phase  $\phi_i$ , and the time instant each leg leaves and returns to contact with the ground. From these results, and knowing  $T$ ,  $\beta$  and  $t_s$ , the  $\{x, y\}$  trajectory of the tip of the foot must be completed during  $t_T$ .

For each cycle the  $\{x, y\}$  trajectory of the tip of the swing leg is computed through a cycloid function given by (considering that the transfer phase starts at  $t = 0$  sec for leg 1), with  $f = 1/T$ :

- during the transfer phase:

$$x_{F1}(t) = V_F \left[ t - \frac{1}{2\pi f} \sin(2\pi f t) \right] \quad (2a)$$

$$y_{F1}(t) = \frac{F_C}{2} [1 - \cos(2\pi f t)] \quad (2b)$$

- during the stance phase:

$$x_{F1}(t) = V_F \left[ T - \frac{1}{2\pi f} \sin(2\pi f T) \right] = V_F T \quad (3a)$$

$$y_{F1}(t) = 0 \quad (3b)$$

Based on this data, the trajectory generator is responsible for producing a motion that synchronises and co-ordinates the legs.

In order to avoid the impact and friction effects we impose null velocities of the feet in the instants of landing and taking off, assuring also the velocity continuity. These joint trajectories can be accomplished also with a step or a polynomial acceleration time profile. After planning the joint trajectories we calculate the inverse dynamics in order to map the kinematics into power consumption.

The dynamic equations for the walking robot are of the form:

$$\boldsymbol{\tau} = \mathbf{H}(\boldsymbol{\theta})\ddot{\boldsymbol{\theta}} + \mathbf{c}(\boldsymbol{\theta}, \dot{\boldsymbol{\theta}}) + \mathbf{g}(\boldsymbol{\theta}) \quad (4)$$

where  $\boldsymbol{\tau}$  is the  $n \times 1$  vector of actuator torques,  $\boldsymbol{\theta}$  is the  $n \times 1$  vector of joint coordinates,  $\mathbf{H}(\boldsymbol{\theta})$  is the  $n \times n$  inertia matrix,  $\mathbf{c}(\boldsymbol{\theta}, \dot{\boldsymbol{\theta}})$  is the  $n \times 1$  vector of centrifugal/Coriolis torques and  $\mathbf{g}(\boldsymbol{\theta})$  is the  $n \times 1$  vector of gravitational torques.

### 3 MEASURES FOR PERFORMANCE EVALUATION

In this section it is analysed the robot dynamic walking. In mathematical terms, we provide several global measures of the overall dexterity of the mechanism in an average sense (10,11). The aim is to verify whether a correlation between different viewpoints can be found in walking.

### 3.1 Mean Absolute Power

The key measure in this analysis is the mean absolute power. It is computed assuming that power regeneration is not available by motors doing negative work, that is, by taking the absolute value of the power. At a given joint  $j$  (each leg has  $m = 3$  joints) and leg  $i$  (since we are studying a hexapod,  $n = 6$  legs), the mechanical power is the product of the motor torque and angular velocity. The global index is obtained by averaging the mechanical absolute power delivered over a period  $T$ :

$$P_{av} = \frac{1}{T} \sum_{i=1}^n \sum_{j=1}^m \int_0^T |\boldsymbol{\tau}_{i,j}(t) \cdot \dot{\boldsymbol{\theta}}_{i,j}(t)| dt \quad (5)$$

where  $\boldsymbol{\tau}$  is the motor torque and  $\dot{\boldsymbol{\theta}}$  is the angular velocity of the joint under consideration. The average power consumption should be minimised and, by consequence,  $P_{av}$ .

### 3.2 Mean Power Dispersion

Although minimising power appears to be an important consideration, it may occur an instantaneous near-infinite power demand. In such a case, the average value can be small while the peak is physically unrealisable. An alternative index is the standard deviation that evaluates the dispersion around the mean absolute power over a complete cycle  $T$ :

$$P_i(t) = \sum_{i=1}^n \sum_{j=1}^m \boldsymbol{\tau}_{i,j}(t) \cdot \dot{\boldsymbol{\theta}}_{i,j}(t) \quad (6a)$$

$$D_{av} = \sqrt{\frac{1}{T} \int_0^T (P_i(t) - P_{av})^2 dt} \quad (6b)$$

where  $P_i$  is the total instantaneous mechanical power. In this perspective, the most suitable trajectory is, also, the one that minimizes  $D_{av}$ .

### 3.3 Mean Power Lost

Another optimisation strategy for an actuated system considers the energy lost in the joint actuators. In this perspective, the index mean power lost can be defined as:

$$P_L = \frac{1}{T} \sum_{i=1}^n \sum_{j=1}^m \int_0^T (\boldsymbol{\tau}_{i,j}(t))^2 dt \quad (7)$$

Once again, the most suitable trajectory is the one that minimizes  $P_L$ .

## 4 SIMULATION RESULTS

To illustrate the use of the preceding concepts, in this section we describe a set of experiments developed, to estimate the influence of several parameters during periodic gaits and to compare the performance measures.

Gaits describe discontinuous sequences of collective leg movements, alternating between transfer and support phases and, in the simulations, we consider the Wave gait, Equal Phase Half Cycle gait, Equal Phase Full Cycle gait, Backward Wave gait, Backward Equal Phase

Half Cycle gait and Backward Equal Phase Full Cycle gait { *WG*, *EPHC*, *EPFC*, *BW*, *BEPHC*, *BEPFC* } (1).

During the experiments, we examine the role of the walking gait versus  $\beta$ ,  $L_S$ ,  $H_B$  and  $F_C$ , with  $L_1 = L_2 = 1$  m,  $M_1 = M_2 = 1$  Kg,  $M_b = 36$  Kg,  $M_f = 0$  Kg and  $S_P = 1$  m. Furthermore, we start with the Wave Gait and then we examine the variation of the indices with other periodic walking patterns.

#### 4.1 Duty Factor vs. Step Length

From Figure 2 we can conclude that  $P_{av}$  and  $D_{av}$  increase monotonically with  $\beta$  and  $L_S$ .

On the other hand,  $P_L$  increases with  $L_S$ , but the variation is almost negligible for low values of  $\beta$ . For values of  $L_S$  below 0.6 m,  $P_L$  decreases with  $\beta$ , until  $\beta \approx 80\%$ , but increases again for higher values of  $\beta$ . For values of  $L_S$  above 0.8 m,  $P_L$  increases monotonically with  $\beta$ .

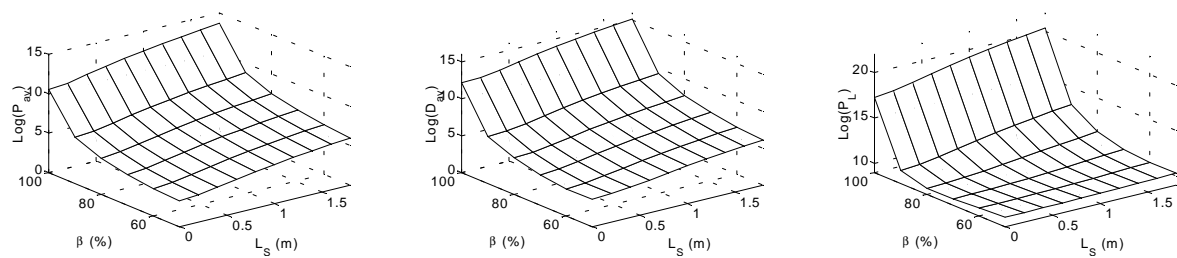


**Fig. 2** Plots of  $P_{av}$ ,  $D_{av}$  and  $P_L$  vs. ( $\beta$ ,  $L_S$ ) for  $F_C = 0.2$  m,  $H_B = 1.6$  m, *WG*

#### 4.2 Duty Factor vs. Foot Clearance

Figure 3 shows that  $P_{av}$  and  $D_{av}$  present the same type of variation with  $\beta$  and  $F_C$ . Specifically, both indices increase with  $\beta$  and  $F_C$ . Moreover, we can observe that  $P_L$  increases monotonically with  $\beta$ , for  $F_C > 0.8$  m. For  $F_C < 0.8$  m,  $P_L$  decreases with  $\beta$ , while  $\beta < 80\%$ , and then increases for  $80\% < \beta < 100\%$ . Regarding the variation with  $F_C$ , we conclude that  $P_L$  increases monotonically.

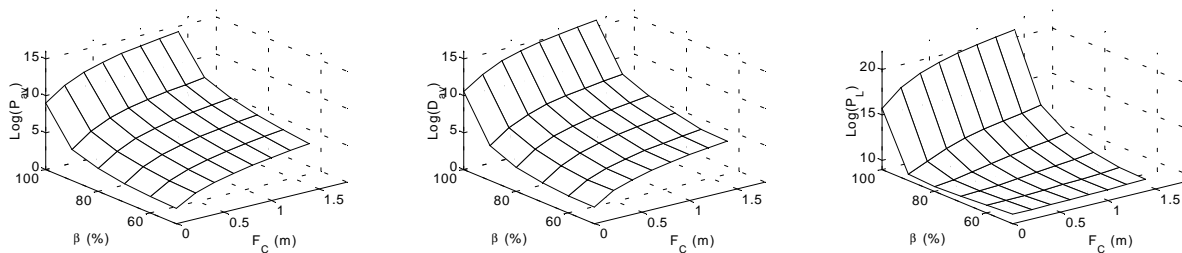


**Fig. 3** Plots of  $P_{av}$ ,  $D_{av}$  and  $P_L$  vs. ( $\beta$ ,  $F_C$ ) for  $L_S = 0.2$  m,  $H_B = 1.6$  m, *WG*

#### 4.3 Duty Factor vs. Body Height

From Figure 4 we observe that the dynamic indices present the same type of variation with  $\beta$  and  $H_B$ , namely, all indices increase with  $\beta$  and decrease slightly with  $H_B$ .

Regarding  $P_L$ , for  $F_C < 0.4$  m and  $L_S < 0.4$  m,  $P_L$  decreases with  $\beta$ , for  $50\% < \beta < 80\%$ , and then increases for  $80\% < \beta < 100\%$ .

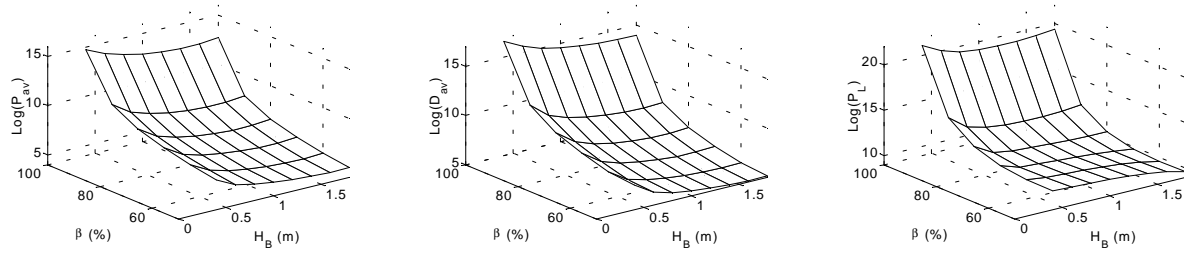


**Fig. 4** Plots of  $P_{av}$ ,  $D_{av}$  and  $P_L$  vs. ( $\beta$ ,  $H_B$ ) for  $F_C = 0.2$  m,  $L_S = 1$  m,  $WG$

#### 4.4 Step Length vs. Body Height

Figure 5 shows that  $P_{av}$  and  $D_{av}$  decrease slightly with  $H_B$ , and increase with  $L_S$ . On the contrary,  $P_L$  decreases with  $H_B$ , and increases only slightly with  $L_S$ .

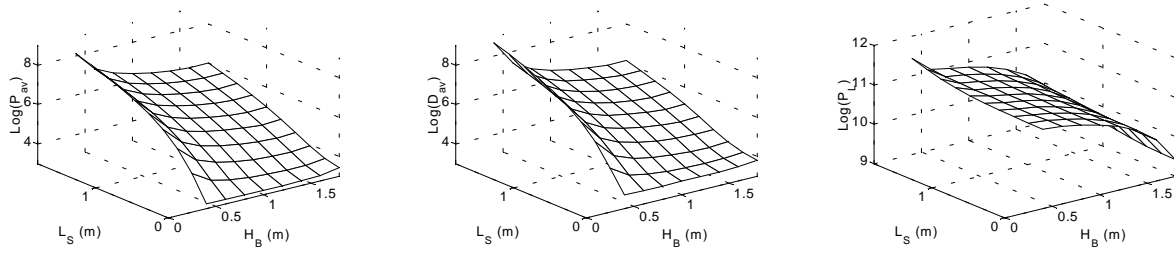


**Fig. 5** Plots of  $P_{av}$ ,  $D_{av}$  and  $P_L$  vs. ( $L_S$ ,  $H_B$ ) for  $\beta = 50\%$ ,  $F_C = 0.2$  m,  $WG$

#### 4.5 Foot Clearance vs. Body Height

Figure 6 shows that  $P_{av}$  and  $D_{av}$  decrease with  $H_B$ , until  $H_B < 1.4$  m. Then, for  $H_B > 1.4$  m the indices remain almost constant. These same indices increase monotonically with  $F_C$ . Regarding  $P_L$ , it decreases with  $H_B$  and presents a slightly increase with  $F_C$  (specially for  $H_B > 1.0$  m)

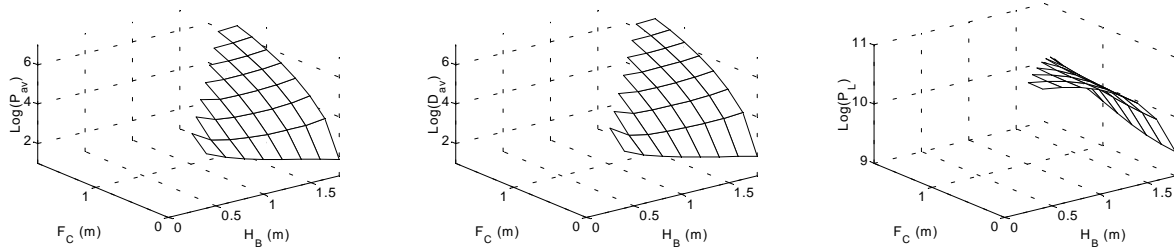


**Fig. 6** Plots of  $P_{av}$ ,  $D_{av}$  and  $P_L$  vs. ( $F_C$ ,  $H_B$ ) for  $\beta = 50\%$ ,  $L_S = 0.2$  m,  $WG$

Comparing all the experiments, we can find a compromise and conclude that for the  $WG$  the best situation occurs for  $\beta \approx 50\%$ ,  $1.6 \leq H_B \leq 1.8$  m,  $L_S < 0.2$  m and  $F_C < 0.1$  m.

#### 4.6 Power Consumption vs. Walking Gaits

Concerning the different periodic walking gaits under study we observed that the proposed indices present the same variation with the parameters  $\beta$ ,  $H_B$ ,  $L_S$  and  $F_C$ . Therefore, we need a complementary analysis in order to compare the performance of different walking gaits.

For this reason, we study the power consumption ( $P_C$ ) along one period of the robot walking cycle, for several gaits. In this line of thought, Figure 7 reveals that the  $EPHC$  and  $EPFC$  require a peak of  $P_C$  lower than the  $WG$ .

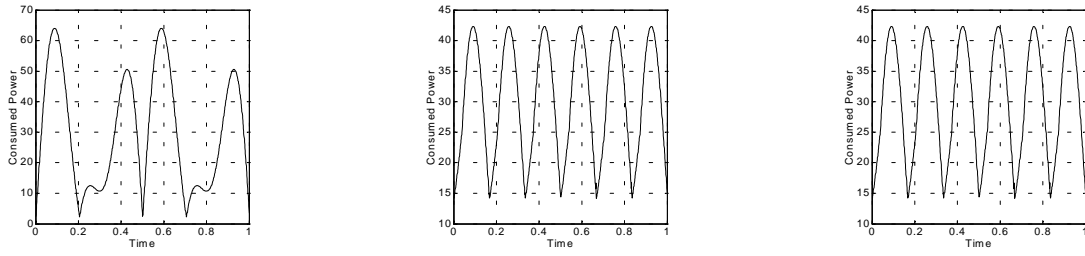


**Fig. 7** Plots of  $P_C$  for  $\beta = 50\%$ ,  $H_B = 1.6$  m,  $F_C = 0.2$  m,  $L_S = 0.2$  m, *WG*, *EPHC*, *EPFC*

Since the  $P_C$  variation vs. time for the backward gaits is similar to those of the forward gaits, we conclude that the *WG* is less efficient than the *EPHC* and the *EPFC*, from the viewpoint of an autonomous energy source.

On Figure 8 we compare the  $P_C$  of the left and right sides of the robot. All gaits present similar requirements on both sides, but for this situation, the *EPFC* gait presents the lowest power peak. Moreover, both forward and backward gaits are similar in this perspective.

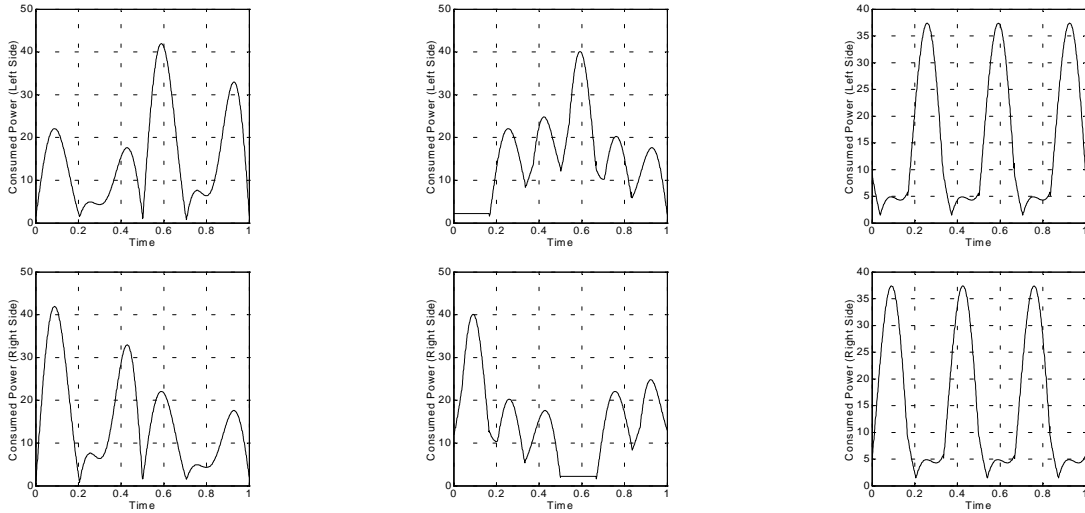


**Fig. 8** Plots of  $P_C$  of the left and right sides of the robot for  $\beta = 50\%$ ,  $H_B = 1.6$  m,  $F_C = 0.2$  m,  $L_S = 0.2$  m, *WG*, *EPHC*, *EPFC*

We also compared  $P_C$  on the front and back legs, and concluded that, in this perspective, there is no difference with the walking gait.

Finally, Figure 9 presents  $P_C$  for the *WG*, with  $\beta = 90\%$ . Comparing the chart with Figure 7, we conclude that the  $P_C$  increases with  $\beta$ , as we noted previously.

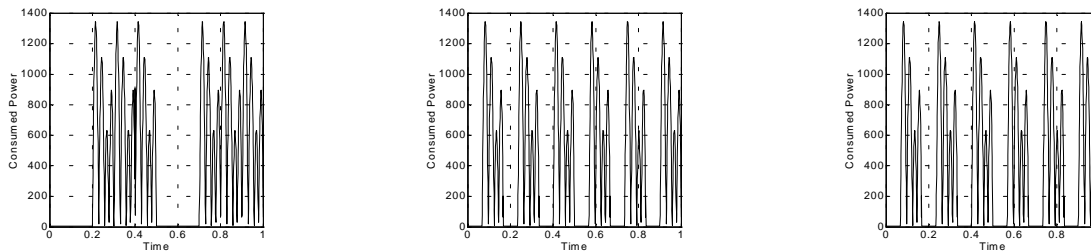


**Fig. 9** Plots of  $P_C$  for  $\beta = 90\%$ ,  $H_B = 1.6$  m,  $F_C = 0.2$  m,  $L_S = 0.2$  m, *WG*, *EPHC*, *EPFC*

## 5 CONCLUSIONS

In this paper we have compared various dynamic aspects of multi-legged robot locomotion gaits. By implementing different motion patterns, we estimated how the robot responds to a variety of locomotion variables such as duty factor, step length, body height, and maximum foot clearance. Three quantitative measures were formulated for analysing the dynamic performance namely the Average Power Consumption, the Power Consumption Standard Deviation and the Power Expenditure in the Electrical Motors. Through the analysis of the results of the simulations we draw some conclusions on the best set of locomotion variables, from a power point of view.

While our focus has been on 2D legged locomotion, certain aspects of locomotion are not necessarily captured by the proposed measures. Consequently, future work in this area will address the refinement of our models to incorporate more unstructured terrains, where legged systems should come into their own, as well as analysing the energy requirements for walking machines and compare these with other wheeled and tracked vehicles.

## REFERENCES

- (1) S.-M. Song, K.J. Waldron, *Machines that Walk: The Adaptive Walking Vehicle*, The MIT Press, 1989.
- (2) D. J. Manko, *A General Model of Legged Locomotion on Natural Terrain*, Kluwer, Westinghouse Electric Corporation, 1992.
- (3) M. A. Jiménez, P. G. Santos, "Terrain-Adaptive Gait for Walking Machines", *The International Journal of Robotics Research*, Vol. 16, n. 3, pp. 320-339, 1997.
- (4) S. T. Venkataraman, "A Model of Legged Locomotion Gaits", *IEEE International Conference on Robotics and Automation*, Minneapolis, USA, 1996.
- (5) David Wettergreen, Chuck Thorpe, "Gait Generation for Legged Robots", *1992 IEEE International Conference on Intelligent Robots and Systems*, July 1992.
- (6) David Wettergreen, Henning Pangels, Jonh Bares, "Behavior-based Gait Execution for the Dante II Walking Robot", *1995 IEEE International Conference on Intelligent Robots and Systems*, Pittsburgh, PA, 7-9 August 1995.
- (7) P. Gregorio, M. Ahmadi and M. Buehler, "Design, Control, and Energetics of an Electrically Actuated Legged Robot", *IEEE Transactions on Systems, Man and Cybernetics*, Vol. 27, n. 4, 1997.
- (8) Lapshin, V. V., "Energy Consumption of a Walking Machine. Model Estimations and Optimization", *ICAR'95 - IEEE International Conference on Advanced Robotics*, Budapest, Hungary, 1995, pp. 420-425.
- (9) Manuel F. Silva, J. A. Tenreiro Machado, António M. Lopes, "Performance Analysis of Periodic Gaits in Multi-Legged Locomotion", *ICAR'01 - IEEE International Conference on Advanced Robotics*, Budapest, Hungary, 2001.
- (10) Filipe M. Silva, J. A. Tenreiro Machado, "Towards Efficient Biped Robots", *1998 IEEE International Conference on Intelligent Robots and Systems*, Victoria, Canada, October 13-17, 1998.
- (11) Filipe M. Silva, J. A. Tenreiro Machado, "Energy Analysis During Biped Walking", *IEEE International Conference on Robotics and Automation*, Detroit, Michigan, USA, 1999.